Petroleum Science 20 (2023) 2479–2487

Contents lists available at ScienceDirect

Petroleum Science

journal homepage: www.keaipublishing.com/en/journals/petroleum-science

Original Paper

Experimental investigation on the effective thermal conductivities of different hydrate-bearing sediments

Xingxun Li [a, *], Rucheng Wei [a], Qingping Li [b, **], Weixin Pang [b], Qi Fan [b], Guangjin Chen [a], Changyu Sun [a]

[a] State Key Laboratory of Heavy Oil Processing, China University of Petroleum-Beijing, Beijing, 102249, China
[b] State Key Laboratory of Natural Gas Hydrate, CNOOC Research Institute Co., Ltd., Beijing, 100027, China

ARTICLE INFO

Article history:
Received 29 August 2022
Received in revised form
1 November 2022
Accepted 17 February 2023
Available online 18 February 2023

Edited by Jia-Jia Fei

Keywords:
Hydrate
Thermal conductivity
Sediment
Heat transfer
In-situ measurement

ABSTRACT

The natural gas hydrate has been regarded as an important future green energy. Significant progress on the hydrate exploitation has been made, but some challenges are still remaining. In order to enhance the hydrate exploitation efficiency, a significant understanding of the effective thermal conductivity (ETC) of the hydrate-bearing sediment has become essential, since it directly controls the heat and mass transfer behaviors, and thereby determines the stability of hydrate reservoir and production rate. In this study, the effective thermal conductivities of various hydrate-bearing sediments were *in-situ* measured and studied. The impacts of temperature, particle size and type of sediment were investigated. The effective thermal conductivities of the quartz sand sediments before and after hydrate formation were *in-situ* measured. The results show the weak negative correlation of effective thermal conductivity of the quartz sand sediment on the temperature before and after the hydrate formation. The effective thermal conductivity of the hydrate-bearing sediment decreases with the increase of particle size of the sediment. The dominant effect of the type of porous medium on the characteristics of the effective thermal conductivity of hydrate-bearing sediment was highlighted. The results indicate that both the effective thermal conductivities of hydrate-bearing quartz sand sediment and hydrate-bearing silicon carbide sediment are weakly negatively correlated with temperature, but the effective thermal conductivity of hydrate-bearing clay sediment is weakly positively dependent on the temperature. In addition, the values of the effective thermal conductivities of various hydrate-bearing sediments are in the order of hydrate-bearing silicon carbide sediment > hydrate-bearing quartz sand sediment > hydrate-bearing clay sediment. These findings could suggest that the intrinsic thermal conductivity of porous medium could control the characteristics of effective thermal conductivity of hydrate-bearing sediment.

1. Introduction

The natural gas hydrate has been identified as the one of the most promising future clean energy sources (Yin and Linga, 2019). The hydrate exploitation in the South China Sea has achieved significant progress and faced challenges (Qin et al., 2022; Xu et al., 2022). The exploitation of the natural gas hydrate mainly involves mass transfer, heat transfer and gas-liquid phase flow processes. The multiphase flow transport, heat and mass transfer are of importance on the natural gas recovery coupled with the thermal-hydraulic-chemical-mechanical (THCM) process (Zhang et al., 2022). The thermophysical property data of hydrate is of significance (Jr and Koh, 2007; Sun et al., 2022). The heat transfer process and thermal property of hydrate deposits are critical to evaluate the stability of hydrate reservoir and determine the production efficiency of natural gas hydrate (Kim and Yun, 2013; Li et al., 2022; Muraoka et al., 2015; Rosenbaum et al., 2007; Sun et al., 2019; Yang et al., 2015, 2016; Yin et al., 2020). The increases in the thermal diffusivity and thermal conductivity of the hydrate dissociated region could lead to the higher dissociation rate (Yin et al., 2016). Therefore, the investigation of the heat transfer characteristics of the hydrate-bearing sediment can provide important fundamental data for the hydrate exploitation (Kanda et al., 2020; Liu et al., 2019;

* Corresponding author.
** Corresponding author.
E-mail addresses: lixingxun@cup.edu.cn (X. Li), liqp@cnooc.com.cn (Q. Li).

https://doi.org/10.1016/j.petsci.2023.02.016

Song et al., 2016; Wan et al., 2018; Zhang et al., 2021). The effective thermal conductivity (ETC) is one of the important thermophysical properties of hydrate-bearing sediment, which has a predominant impact and an effective indication on the heat transfer process of hydrate-bearing sediment (Wei et al., 2022), hence directly controlling the heat transfer rate (Zhang et al., 2022), and energy efficiency during the hydrate exploitation (Wu et al., 2022). Therefore, it is of great significance to investigate the effective thermal conductivity of hydrate-bearing sediment to provide a better understanding of hydrate exploitation process and hence improve the production efficiency.

The thermal conductivity of hydrate sediment has been recently measured and studied by using different experimental methods and in various systems, but the knowledge related to its evolution considering some significant factors still remains limited. Wei et al. (2022) used a point-heat-source device to measure the effective thermal conductivity of methane hydrate-bearing clay sediment, considering the impact of phase transition including the ice melting and hydrate formation and dissociation. They found that the effective thermal conductivity increased during the hydrate formation, but decreased when the ice was melted and the hydrate was decomposed (Wei et al., 2022). He et al. (2021b) employed the transient hot-wire approach to measure the effective thermal conductivity of hydrate-bearing quartz sands, and investigated the impacts of gas/water saturation, gas pressure/temperature and hydrate distribution. Wei et al. (2021) reported the effect of compaction on the effective thermal conductivity of natural marine sediment containing hydrate and confirmed the increase of its effective thermal conductivity resulted from the decreased porosity of the sediment. They presented that the porous structure variation caused by the icing and hydrate reformation leaded to the change of the effective thermal conductivity (Wei et al., 2021). Sun et al. (2019) used the transient plane source (TPS) technique to measure the dependence of thermal conductivities of high-quality methane hydrate sample and methane hydrate-bearing seasand on the temperature. They proposed that the thermal conductivities of methane hydrate and methane hydrate-bearing seasand had positive correlations with the temperature (Sun et al., 2019). However, Li and Liang (2016) measured the effective thermal conductivity of methane hydrate-bearing quartz sand, confirmed the weak negative dependence of effective thermal conductivity on the temperature, and stated the significant effect of morphology on the thermal conductivity of sediment. He et al. (2021a) measured the effective thermal conductivity of the hydrate-bearing quartz sand during the depressurization, and highlighted the significance of hydrate dissociation and grain rearrangement. Chuvilin and Bukhanov (2017) investigated the impact of hydrate formation on the thermal conductivity of gas-saturated sediment and presented that the variation of thermal conductivity could be caused by the change of pore space condition due to hydrate formation. The experimental methods for thermal conductivity measurement of hydrate-bearing sediment, material and particle size of sediments used in these studies are summarized in Table 1.

Even though the effective thermal conductivities of the sediments containing hydrate have been recently measured and studied in literatures, the investigations of the influences of the phase transition, particle size, type of porous sediment on the effective thermal conductivity have been still insufficient. Especially, the significance of the role of the sediment type and its intrinsic thermal conductivity on the effective thermal conductivity of hydrate-bearing sediment have been rarely highlighted. Hence, in this study, the effective thermal conductivities of different hydrate-bearing sediment samples with various types of porous sediments, hydrates, and different sizes of sediment particle were *in-situ* measured and investigated at different temperatures. This work could contribute to improving and enriching the fundamentals and database of thermophysical properties of various hydrate-bearing sediments, and hence gaining better understanding of the heat transfer phenomenon during hydrate exploitation process.

2. Experimental section

2.1. Materials

As a substitute for natural gas hydrate, TBAB (tetrabutylammonium bromide) hydrate and cyclopentane hydrate can be formed under moderate conditions under atmospheric pressure. Moreover, TBAB hydrate and cyclopentane hydrate are similar to natural gas hydrate in many physical properties. Thus, in this study, the TBAB hydrate-bearing sediments and cyclopentane hydrate-bearing sediments were prepared and used for the *in-situ* measurement of effective thermal conductivity of hydrate-bearing sediment. Three kinds of sediment particles were used, which are clay ($Al_2O_3 \cdot 4SiO_2 \cdot nH_2O$, $\geq$ 95%, 200–300 mesh), quartz sand (SiO_2, $\geq$ 95%, 20–40 mesh, 80–120 mesh and 200–300 mesh) and silicon carbide (SiC, $\geq$ 95%, 200–300 mesh). The hydrate-bearing sediments in the South China Sea are widely identified as clay-rich type of sediment, and the clay minerals have effects on the hydrate formation and dissociation (Ren et al., 2022). Hence, the clay particles were used in this study. The particle size distribution curve of the clay was measured by the particle size analyzer (Malvern Mastersizer, 2000) and shown in Fig. 1. The effective thermal conductivities of six types of hydrate-bearing sediments were studied, which are TBAB hydrate-bearing clay, quartz sand, silicon carbide sediments and cyclopentane hydrate-bearing clay, quartz sand, silicon carbide sediments. In order to investigate the effect of sediment particle size on the effective thermal conductivity of hydrate-bearing sediment, three different sizes of quartz sand particles were used, which were 20–40 mesh, 80–120 mesh and 200–300 mesh.

For the homogeneous TBAB hydrate-bearing sediment preparation, the 42 wt% TBAB aqueous solution was first prepared, and then the sediment particles were completely saturated with the TBAB aqueous solution. Finally, the TBAB hydrate (phase equilibrium temperature: ~12 °C) was formed under the condition that the water bath temperature was 0.3 °C (to avoid the formation of ice). For the preparation of cyclopentane hydrate-bearing sediment, the cyclopentane and water were first emulsified with the span 80 to form a stable and uniform emulsion (the mass ratio of water to cyclopentane was 1.4:1), then the sediment particles were then completely saturated with the emulsion, and finally cyclopentane hydrate (phase equilibrium temperature: 7.1 °C) was formed under the condition of water bath temperature of 0.3 °C.

2.2. Methods

Fig. 2 shows the schematic diagram of *in-situ* thermal conductivity measurement system of hydrate-bearing sediment used in this study. This experimental setup mainly includes the thermal conductivity measurement system, temperature control system and hydrate formation system. The thermal conductivity measurement system includes the thermal conductivity measurement instrument host (TC 4000E) and the thermal conductivity probe sensor. The probe sensor is composed of thermocouple, heating wire and stainless steel needle tube, the diameter of the probe sensor is 3 mm, and the total length is 120 mm. This system was mainly used to *in-situ* measure and record the effective thermal conductivity of hydrate-bearing sediment. The thermal probe method for thermal conductivity measurement is based on the principle of the hot wire method.

Table 1
Summary of effective thermal conductivity measurements of hydrate-bearing sediments in literatures (Chuvilin and Bukhanov, 2017; He et al., 2021a, 2021b; Li and Liang, 2016; Sun et al., 2019; Wei et al., 2021, 2022).

Work	Experimental test method	Porous media	Particle size
Li and Liang (2016)	Transient plane source (TPS)	Quartz sand	250–425 μm
Chuvilin and Bukhanov (2017)	Thermocouple heating	Sand, silty sand, kaolin	Grain size fraction: Sand-1 (1–0.05 mm: 94.8%, 0.05–0.001 mm: 3.1%, < 0.001 mm: 2.1%) Sand-2 (1–0.05 mm: 82.3%, 0.05–0.001 mm: 12.7%, < 0.001 mm: 2.7%) Silty sand (1–0.05 mm: 41.8%, 0.05–0.001 mm: 53.7%, < 0.001 mm: 4.5%) Kaolin (1–0.05 mm: 4.5%, 0.05–0.001 mm: 70.9%, < 0.001 mm: 24.6%)
Sun et al. (2019)	Transient plane source (TPS)	Natural seasand	Volume percentage: < 4 μm: 0%, 4–63 μm: 0%, 63–250 μm: 22.173%, 250–500 μm: 77.827%, 500–2000 μm: 0%, > 2000 μm: 0%
He et al. (2021a)	Transient hot-wire method	Quartz sand	100–120 mesh
He et al. (2021b)	Transient hot-wire method	Quartz sand	100–120 mesh
Wei et al. (2021)	Point-heat-source based measurement	Marine sediment grain	0.5–140 μm
Wei et al. (2022)	Point-heat-source based measurement	Montmorillonite, marine sediment	Montmorillonite: D50 = 8.892 μm, marine sediment: D50 = 7.835 μm

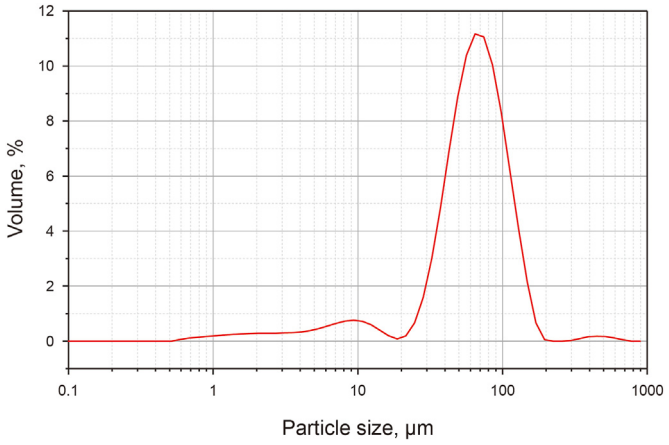

Fig. 1. The particle size distribution curve of the clay.

Under the assumption of isotropy, the radius of the thermal probe is small and the heat loss in the measurement process could be ignored. The thermal conductivity model is transformed into a one-dimensional heat transfer process to derive the thermal conductivity. The hydrate-bearing sediment samples used in this work were *in-situ* formed in the hydrate formation cell, as shown in Fig. 2. The temperature control system includes a constant-temperature cooling water bath (DCW-4006) and temperature transducer (WZP-PT100). All of the hydrate formation cell, hydrate-bearing sediment, thermal conductivity probe sensor and temperature transducer were immersed in the cooling water bath to ensure the constant measurement temperature.

2.3. Formation and growth characteristics of TBAB hydrate and TBAB hydrate-bearing sediment

The formation of TBAB hydrate is an exothermic process, which could lead to the rapid rise of temperature in the hydrate simulator, so the rapid rise of temperature can be used to describe the formation and growth behaviors of the hydrate. The temperature profile of the TBAB hydrate formation process is shown in Fig. 3a. Although the temperature of TBAB aqueous solution (42 wt%) was reduced to below the phase equilibrium temperature (Fig. 3a), but the TBAB hydrate was not formed immediately, and there was an induction period of about 2 h. The temperature in the hydrate simulator then increased rapidly. This means that the TBAB hydrate began to be formed. After the temperature reaching the highest point, the TBAB hydrate was continuously formed and accompanied with the gradual reduction of the TBAB hydrate formation rate and heat release in the formation process. Meanwhile, under the refrigeration of the external water bath, the heat released in the hydrate formation process was gradually transferred to the external environment, resulting in the gradual decline of the temperature in the hydrate simulator, and finally the temperature was reduced to the system temperature. This stage is the hydrate formation stage lasting for about 700 min. After the hydrate formation stage, the temperature in the hydrate simulator finally tends to stabilize, as

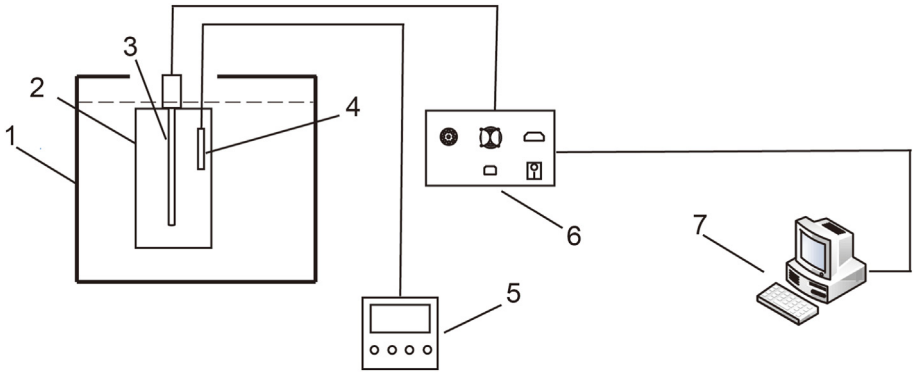

Fig. 2. Schematic diagram of *in-situ* thermal conductivity measurement system of hydrate-bearing sediment ((1) constant-temperature cooling water bath, (2) hydrate formation cell, (3) thermal conductivity probe sensor, (4) temperature transducer, (5) data acquisition, (6) thermal conductivity measurement instrument host, (7) computer).

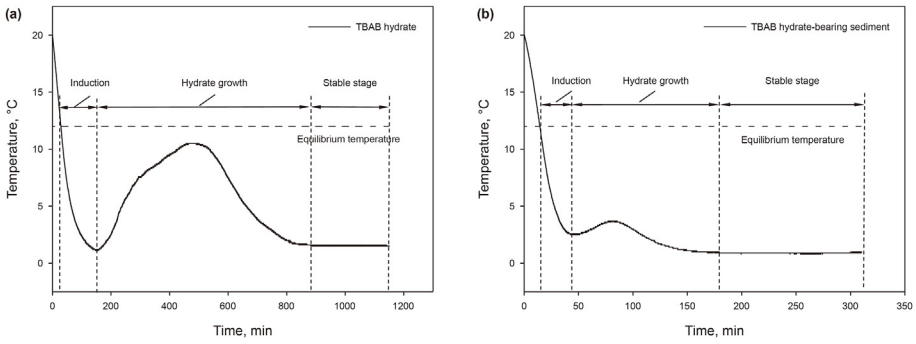

Fig. 3. Temperature variation profiles during the formations of (**a**) TBAB hydrate and (**b**) TBAB hydrate-bearing quartz sand sediment with the particle size of 80–120 mesh.

shown in the stable stage in Fig. 3a. In order to ensure the accuracy and stability of the subsequent measurement of the thermal conductivity of the TBAB hydrate, the temperature water bath was kept unchanged for 48 h after the completion of the TBAB hydrate formation. Fig. 3b shows the temperature variation profile during the formation TBAB hydrate-bearing sediment. It can be seen from Fig. 3b that the induction time of TBAB hydrate in the porous medium (quartz sand sediment) is less than 50 min. It was significantly shortened, compared with the one for TBAB hydrate (Fig. 3a). The quartz sands can effectively shorten the induction time of TBAB hydrate.

3. Results and discussion

3.1. Effective thermal conductivities of water-saturated sediment and ice-bearing sediment

Prior to the investigation on the effective thermal conductivity of hydrate-bearing sediment, the effective thermal conductivities of the water-saturated quartz sand sediment and ice-bearing quartz sand sediment with the particle size of 80–120 mesh were first *in-situ* measured in this work. As shown in Fig. 4a, the effective thermal conductivity of the water-saturated quartz sand sediment is weakly negatively correlated with temperature, in the temperature range of 277.15–307.15 K. Since the ice might form in the hydrate sediment during the hydrate exploitation process, the effective thermal conductivity of the ice-bearing sediment was investigated. As shown in Fig. 4b, the effective thermal conductivities of ice-bearing quartz sand system is larger than the ones of water-saturated quartz sand sediment, and is also weakly negatively correlated with temperature.

In order to investigate the difference of effective thermal conductivities of various water-saturated sediments, the effective thermal conductivities of water-saturated clay sediment, water-saturated quartz sand sediment and water-saturated silicon carbide sediment with the same particle sized of 200–300 mesh were *in-situ* measured in the temperature range of 276.8–303.32 K. As shown in Fig. 5, the effective thermal conductivity of the water-saturated clay sediment is weakly positively correlated with temperature, while both the effective thermal conductivities of water-saturated quartz sand sediment and water-saturated silicon carbide sediment are weakly negatively correlated with temperature. In addition, the value of the effective thermal conductivity of water-saturated silicon carbide sediment is much higher than those of water-saturated clay sediment and water-saturated quartz sand sediment. The effective thermal conductivity of water-saturated quartz sand sediment is higher than the one of water-saturated clay sediment. These are mainly due to the fact that the intrinsic thermal conductivities of the three porous media are different.

3.2. Thermal conductivities of TBAB hydrate and cyclopentane hydrate

In this section, the thermal conductivities of TBAB hydrate under different temperatures were first *in-situ* measured, and compared with the literature values (Fig. 6). It can be seen from Fig. 6 that the thermal conductivity of TBAB hydrate ranges from 0.3741 to 0.3811 W/(m·K) in the temperature range of 258.53–274.94 K, and the thermal conductivity of TBAB hydrate is weakly negatively correlated with temperature.

In the literatures, Fujiura et al. (2016) used a transient hot-wire device to measure the thermal conductivity of TBAB hydrate (TBAB solution concentration was 40.52 wt%), and concluded the weak negative temperature coefficient of the thermal conductivity of semiclathrate hydrate. Nagatomi et al. (2013) used a transient hot-wire method to perform the thermal conductivity measurements

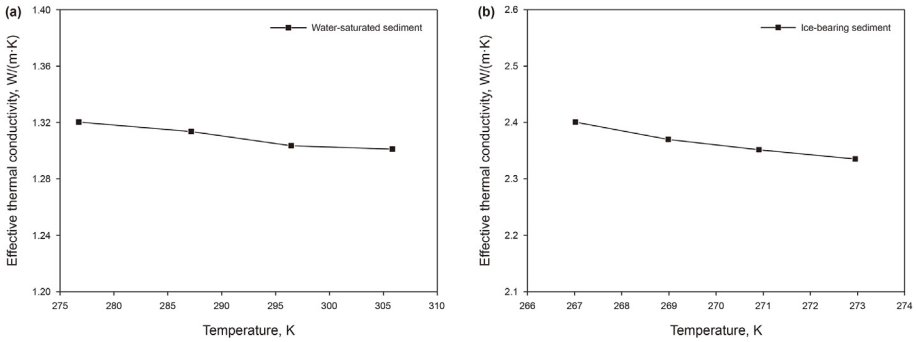

Fig. 4. Effective thermal conductivities of (**a**) water-saturated quartz sand sediment and (**b**) ice-bearing quartz sand sediment with the particle size of 80–120 mesh.

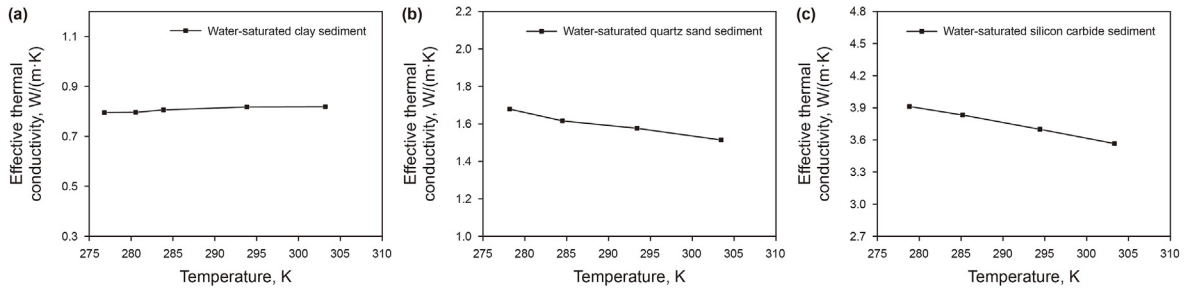

Fig. 5. Effective thermal conductivities of (**a**) water-saturated clay sediment, (**b**) water-saturated quartz sand sediment and (**c**) water-saturated silicon carbide sediment with the particle size of 200–300 mesh.

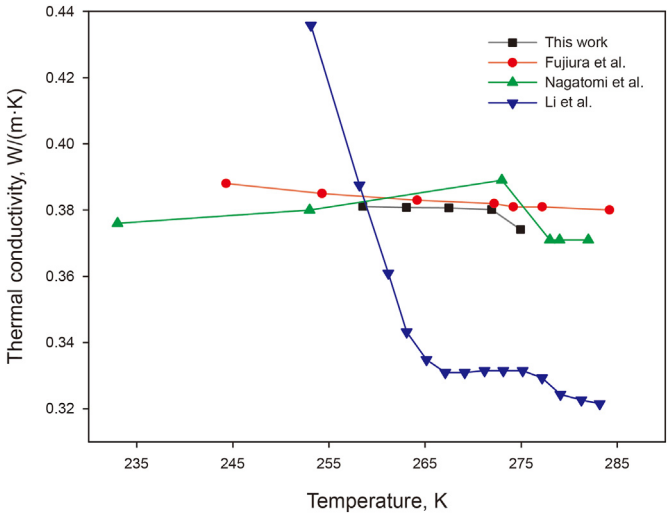

Fig. 6. Experimental data of thermal conductivities of TBAB hydrate and literature values (Fujiura et al., 2016; Li et al., 2016; Nagatomi et al., 2013).

and obtained that the thermal conductivities of TBAB hydrate (TBAB solution concentration was 40 wt%) in the temperature range from 193 to 282 K were within 0.371–0.389 W/(m·K). In the same temperature range, it can be found that the measurement results of thermal conductivity of TBAB hydrate in our experiments are close to those of the literature values. Li et al. (2016) used a single-sided transient plane source technique to measure the thermal conductivity of TBAB hydrate (TBAB solution concentration is 40 wt%) and also found the negative trend of the thermal conductivity of TBAB hydrate with temperature. This was explained by the crystal heat transmission features retained by the TBAB hydrate with a semi-clathrate structure (Li et al., 2016). There are some discrepancies between the experimental values and those in the literatures. This might be mainly due to the different measurement apparatus, methods and solution concentrations used. However, our experimental results in this study are similar to the most of the literature values, and the trend of the dependence of thermal conductivity on the temperature also follows the previous findings. These could confirm the feasibility of the hydrate thermal conductivity measurement apparatus and experimental methodology developed in this study.

The cyclopentane is sparingly miscible with the water and similar to the hydrophobic natural gas, which could form a structure II hydrate (Martinez de Baños et al., 2015; Touil et al., 2017). The cyclopentane hydrate is a well-known model hydrate of practical interest like gas hydrate (Dirdal et al., 2012), since its formation conditions are more readily to reach (Delroisse et al., 2018; Martinez de Baños et al., 2015; Touil et al., 2017). Thus, the cyclopentane hydrate was used as a proper substitute of natural gas hydrate in this study. The thermal conductivities of cyclopentane hydrate at different temperatures were *in-situ* measured in this section, as shown in Fig. 7. The results indicate that the thermal conductivity of cyclopentane hydrate is weakly positively correlated with the temperature in the temperature range of 263.6–275.81 K. Comparing the experimental results in Figs. 6 and 7, it can be found that the thermal conductivity of cyclopentane hydrate is slightly larger than that of TBAB hydrate. This is mainly because the thermal conductivity of hydrate could be related to the structure of hydrate and the size of guest molecules (Andersson and Ross, 1983; Li et al., 2016).

3.3. Effective thermal conductivities of hydrate-bearing sediments and non-hydrate-bearing sediments

In order to investigate the effective thermal conductivities of the hydrate-bearing sediment and non-hydrate-bearing sediment, the effective thermal conductivities of the quartz sand sediments before and after TBAB/cyclopentane hydrate formation were *in-situ* measured as a function of temperature, are shown in Fig. 8a and b. As shown in Fig. 8a, the results indicate that the effective thermal conductivities of the quartz sand sediments before and after TBAB hydrate formation are weakly negatively correlated with the temperature. Other investigations on the effective thermal conductivity of hydrate-bearing quartz sand system also obtain the weak negative dependence of effective thermal conductivity on

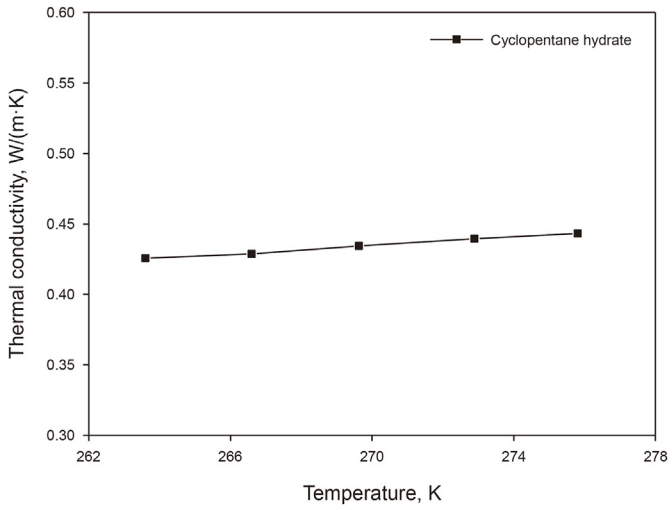

Fig. 7. Thermal conductivities of cyclopentane hydrates at different temperatures.

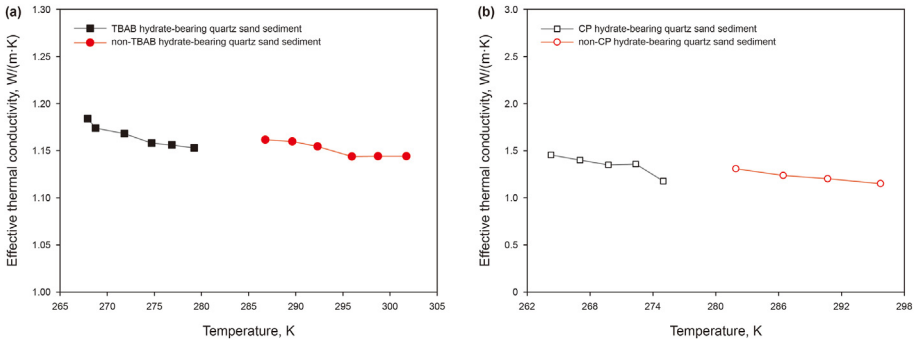

Fig. 8. Effective thermal conductivities of (**a**) TBAB hydrate-bearing sediment and non-TBAB hydrate-bearing sediment, and (**b**) cyclopentane hydrate-bearing sediment and non-cyclopentane hydrate-bearing sediment with the quartz sand particle size of 80–120 mesh.

temperature (Li and Liang, 2016). For the low temperature range, the hydrate formation might cause the increase in the effective thermal conductivity of the hydrate-bearing sediment. The results in literatures obtain these similar findings on the effect of phase transition on the effective thermal conductivity of hydrate-bearing sediment. The hydrate decomposition or ice melting could lead to the declined effective thermal conductivity of hydrate-bearing sediment, but might increase the effective thermal conductivity during hydrate formation (Wei et al., 2022).

In order to confirm the characteristics of the effective thermal conductivities of the sediments before and after the hydrate formation. The effective thermal conductivities of the quartz sand sediments with the particle size of 80–120 mesh before and after cyclopentane hydrate formation were *in-situ* measured, respectively (Fig. 8b). It can be seen from Fig. 8b that the effective thermal conductivity of cyclopentane-water quartz sand sediment before the hydrate formation and cyclopentane hydrate-bearing quartz sand sediment after the hydrate formation are weakly negatively correlated with temperature, and their dependence on the temperature is similar to the one of the effective thermal conductivity of sediments before and after the TBAB hydrate formation (Fig. 8a).

3.4. Effect of particle size of sediment on the effective thermal conductivity of hydrate-bearing sediment

In order to explore the dependence of the effective thermal conductivity of hydrate-bearing sediment on the particle size of sediment, the effective thermal conductivities of TBAB hydrate-bearing quartz sand sediments with the particle sizes of 20–40 mesh, 80–120 mesh and 200–300 mesh were *in-situ* measured. As shown in Fig. 9a, in the temperature range of 265.43–279.23 K, the effective thermal conductivities of TBAB hydrate sediments with three different particle sizes are weakly negatively correlated with temperature. In addition, the effective thermal conductivity of TBAB hydrate-bearing quartz sand sediment with the particle size of 200–300 mesh is the largest, and that of hydrate-bearing sediment with the particle size of 20–40 mesh is the smallest. The results indicate that the effective thermal conductivity of hydrate-bearing sediment decreases with the increase of the particle size of porous medium. This is caused by the larger amount of solid quartz sand in the same volume of quartz sand when the particle size is smaller.

In order to confirm the effect of particle size of sediment on the effective thermal conductivity of hydrate-bearing sediment, the effective thermal conductivities of cyclopentane hydrate quartz sand sediments with the particle sizes of 20–40 mesh, 80–120 mesh and 200–300 mesh were *in-situ* measured in this study, as shown in Fig. 9b. The results indicate that the effective thermal conductivity of the hydrate-bearing quartz sand sediments with three different particle sizes is weakly negatively correlated with the temperature, in the temperature range of 263.45–275.06 K. Within this temperature range, the effective thermal conductivities of cyclopentane hydrate quartz sand sediment of 200–300, 80–120 and 20–40 mesh are 1.5–1.6, 1.18–1.45, and 1.14–1.3 W/(m·K). This shows that the effective thermal conductivity of the cyclopentane hydrate-bearing quartz sand sediment decreases with the increase of particle size, and this variation trend is consistent with those of the TBAB hydrate-bearing quartz sand sediment (Fig. 9a).

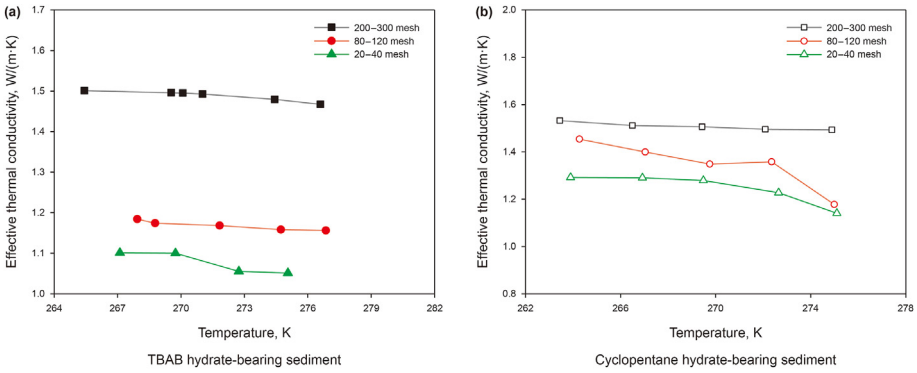

Fig. 9. Effective thermal conductivities of (**a**) TBAB hydrate-bearing quartz sand sediments and (**b**) cyclopentane hydrate-bearing quartz sand sediments with different particle sizes.

3.5. Effect of type of sediment on the effective thermal conductivity of hydrate-bearing sediment

Various porous media have different thermophysical properties, which might affect the effective thermal conductivity of the hydrate-bearing sediment. Therefore, in order to reveal the effect of the type of sediment on the effective thermal conductivity of hydrate-bearing sediment, the effective thermal conductivities of TBAB hydrate-bearing clay sediment, TBAB hydrate-bearing quartz sand sediment and TBAB hydrate-bearing silicon carbide sediment with the particle size of 200–300 mesh were *in-situ* measured, respectively. As shown in Fig. 10a–c, in the temperature range of 264.13–276.60 K, the effective thermal conductivity of TBAB hydrate-bearing clay sediment is weakly positively correlated with temperature, while both the effective thermal conductivities of TBAB hydrate-bearing quartz sand sediment and TBAB hydrate-bearing silicon carbide sediment are weakly negatively correlated with temperature. In addition, the value of effective thermal conductivity of TBAB hydrate-bearing quartz sand sediment is between those of TBAB hydrate-bearing clay sediment and TBAB hydrate-bearing silicon carbide sediment. This is mainly due to the fact that the intrinsic thermal conductivity of silicon carbide is greater than that of quartz sand, but the intrinsic thermal conductivity of quartz sand is greater than that of clay. The effective thermal conductivity of the multiphase sediment can be increased by the porous medium with the higher thermal conductivity (Wang et al., 2017). The trend of the data obtained in this experiment is consistent with the trends of the effective thermal conductivities of the water-saturated clay sediment, water-saturated quartz sand sediment and water-saturated silicon carbide sediment shown in Fig. 5. This also confirms that the intrinsic thermal conductivity of porous medium could dominate the characteristics of thermal conductivity of hydrate-bearing sediment.

The effective thermal conductivities of cyclopentane hydrate-bearing clay sediment, cyclopentane hydrate-bearing quartz sand sediment and cyclopentane hydrate-bearing silicon carbide sediment with the particle size of 200–300 mesh were *in-situ* measured, as shown in Fig. 10d–f. It can be seen from the results that the effective thermal conductivity varies differently with temperature when the porous medium type of sediment changes. In the temperature range of 263.45–275.76 K, the effective thermal conductivity of cyclopentane hydrate-bearing clay sediment is weakly positively correlated with temperature, but the effective thermal conductivities of cyclopentane hydrate-bearing quartz sand sediment and cyclopentane hydrate-bearing silicon carbide sediment are weakly negatively correlated with temperature. The dependence of different cyclopentane hydrate-bearing sediments on the temperature (Fig. 10d–f) is similar to the ones of TBAB hydrate-bearing sediment (Fig. 10a–c). In addition, the effective thermal conductivity values of these three different cyclopentane hydrate-bearing sediments are in the order of hydrate-bearing clay sediment < hydrate-bearing quartz sand sediment < hydrate-bearing silicon carbide sediment. This is because of the different intrinsic thermal conductivities of these three types of water-saturated sediments (Fig. 5). These results in cyclopentane hydrate-bearing sediment also could demonstrate the significance of the type of sediment on the effective thermal conductivity of hydrate-bearing sediment.

The effective thermal conductivities of cyclopentane hydrate-bearing sediments are numerically different from those of TBAB hydrate-bearing sediments. Comparing Fig. 10a–c and Fig. 10d–f, it can be seen that the effective thermal conductivity of TBAB hydrate sediment is smaller than that of cyclopentane hydrate sediment, because the thermal conductivity of cyclopentane hydrate is greater than that of TBAB hydrate. However, the dependence of the effective thermal conductivity of hydrate-bearing sediment on temperature does not change with the variation of the hydrate type. This also might demonstrate that the thermal conductivity of porous medium could dominate the effective thermal conductivity of hydrate-bearing sediment.

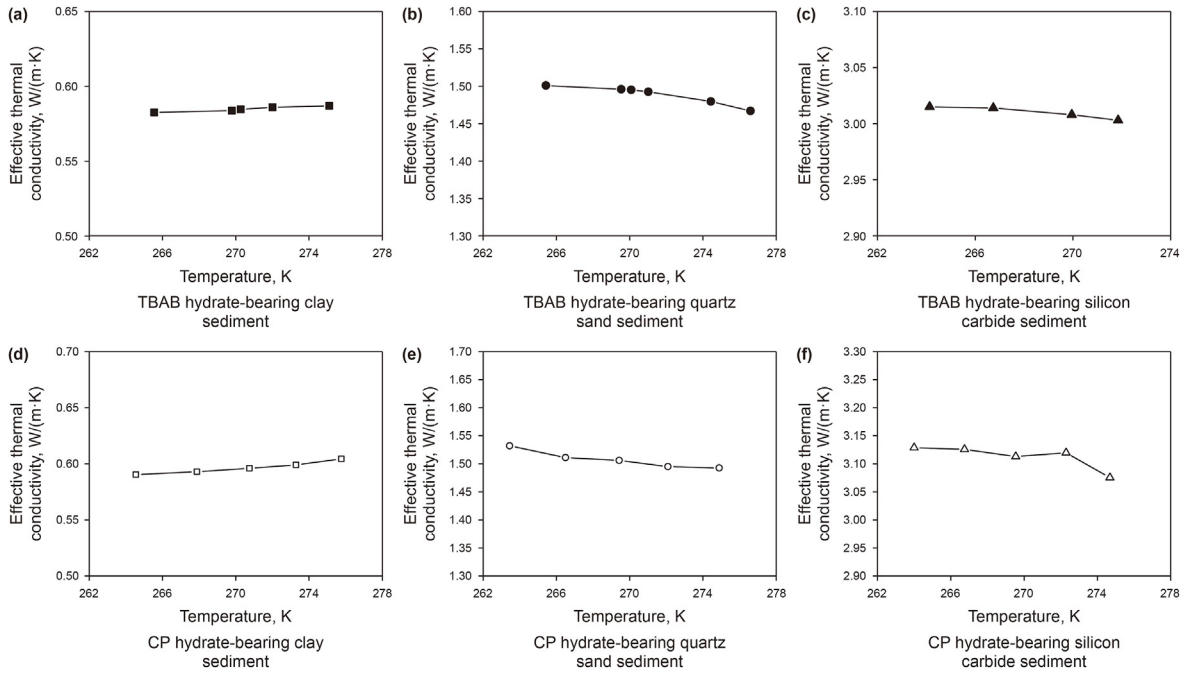

Fig. 10. Effective thermal conductivities of different hydrate-bearing sediments with particle size of 200–300 mesh ((**a**) TBAB hydrate-bearing clay sediment, (**b**) TBAB hydrate-bearing quartz sand sediment, (**c**) TBAB hydrate-bearing silicon carbide sediment, (**d**) cyclopentane hydrate-bearing clay sediment, (**e**) cyclopentane hydrate-bearing quartz sand sediment, (**f**) cyclopentane hydrate-bearing silicon carbide sediment).

4. Conclusions

Due to the significance of the effective thermal conductivity of hydrate-bearing sediment in the controlling the heat transfer behavior of hydrate-bearing sediment, the effective thermal conductivities of different hydrate-bearing sediments (TBAB hydrate-bearing sediment and cyclopentane hydrate-bearing sediment) were directly *in-situ* measured and investigated. The effects of temperature, particle size of sediment, sediment type (clay sediment, quartz sand sediment and silicon carbide sediment) were studied. The effective thermal conductivities of the quartz sand sediments containing hydrate and without hydrate formation were first *in-situ* measured as a function of temperature. The results indicate that the effective thermal conductivities of the quartz sand sediments before and after the hydrate formation are weakly negatively correlated with temperature. The effective thermal conductivity of the hydrate-bearing quartz sand sediment decreases with the increase of particle size of the sediment.

The results from both TBAB hydrate-bearing sediment and cyclopentane hydrate-bearing sediment systems show the weak dependence of effective thermal conductivity on the temperature. The trend of the correlation of effective thermal conductivity of hydrate-bearing sediment could depend on the type of sediment. The results indicate that the effective thermal conductivity of hydrate-bearing clay sediment is weakly positively correlated with temperature, but both the effective thermal conductivities of hydrate-bearing quartz sand sediment and hydrate-bearing silicon carbide sediment are weakly negatively correlated with temperature. Moreover, the effective thermal conductivity values of various hydrate-bearing sediments are in the order of hydrate-bearing clay sediment < hydrate-bearing quartz sand sediment < hydrate-bearing silicon carbide sediment. This is mainly due to the fact of the larger intrinsic thermal conductivity of silicon carbide than that of quartz sand, and the smaller intrinsic thermal conductivity of clay than that of the quartz sand. This study could demonstrate that the dominant effect of the intrinsic thermal conductivity of porous medium on the characteristics of the effective thermal conductivity of hydrate-bearing sediment.

Declaration of competing interest

The authors declare that they have no known competing financial interests or personal relationships that could have appeared to influence the work reported in this paper.

Acknowledgements

This work was supported by the National Natural Science Foundation of China (U19B2005, 21808238, U20B6005, 22127812) and the National Key Research and Development Program of China (2021YFC2800902).

References

Andersson, P., Ross, R.G., 1983. Effect of guest molecule size on the thermal conductivity and heat capacity of clathrate hydrates. J. Phys. C Solid State Phys. 16, 1423–1432. https://doi.org/10.1088/0022-3719/16/8/011.

Chuvilin, E., Bukhanov, B., 2017. Effect of hydrate formation conditions on thermal conductivity of gas-saturated sediments. Energy Fuels 31 (5), 5246–5254. https://doi.org/10.1021/acs.energyfuels.6b02726.

Delroisse, H., Plantier, F., Marlin, L., et al., 2018. Determination of thermophysical properties of cyclopentane hydrate using a stirred calorimetric cell. J. Chem. Therm. 125, 136–141. https://doi.org/10.1016/j.jct.2018.05.023.

Dirdal, E.G., Arulanantham, C., Sefidroodi, H., et al., 2012. Can cyclopentane hydrate formation be used to rank the performance of kinetic hydrate inhibitors? Chem. Eng. Sci. 82, 177–184. https://doi.org/10.1016/j.ces.2012.07.043.

Fujiura, K., Nakamoto, Y., Taguchi, Y., et al., 2016. Thermal conductivity measurements of semiclathrate hydrates and aqueous solutions of tetrabutylammonium bromide (TBAB) and tetrabutylammonium chloride (TBAC) by the transient hot-wire using parylene-coated probe. Fluid Phase Equil. 413, 129–136. https://doi.org/10.1016/j.fluid.2015.09.024.

He, J., Li, X., Chen, Z., et al., 2021a. Effective thermal conductivity changes of the hydrate-bearing quartz sands in depressurization and soaking. J. Nat. Gas Sci. Eng. 89, 103878. https://doi.org/10.1016/j.jngse.2021.103878.

He, J., Li, X., Chen, Z., et al., 2021b. Effect of hydrate distribution on effective thermal conductivity changes during hydrate formation in hydrate-bearing quartz sands. Int. J. Heat Mass Tran. 174, 121289. https://doi.org/10.1016/j.ijheatmasstransfer.2021.121289.

Jr, E.D.S., Koh, C.A., 2007. Clathrate Hydrates of Natural Gases. Crc Press.

Kanda, Y., Komatsu, H., Okajima, J., et al., 2020. Evaluation of rate-determining step of methane hydrate decomposition by measurement of transient heat and mass transfer near solid–gas interface. Int. J. Heat Mass Tran. 149, 119191. https://doi.org/10.1016/j.ijheatmasstransfer.2019.119191.

Kim, Y.J., Yun, T.S., 2013. Thermal conductivity of methane hydrate-bearing Ulleung Basin marine sediments: laboratory testing and numerical evaluation. Mar. Petrol. Geol. 47, 77–84. https://doi.org/10.1016/j.marpetgeo.2013.05.011.

Li, D., Liang, D., 2016. Experimental study on the effective thermal conductivity of methane hydrate-bearing sand. Int. J. Heat Mass Tran. 92, 8–14. https://doi.org/10.1016/j.ijheatmasstransfer.2015.08.077.

Li, D., Liang, D., Peng, H., et al., 2016. Thermal conductivities of methane–methylcyclohexane and tetrabutylammonium bromide clathrate hydrate. J. Therm. Anal. Calorim. 123, 1391–1397. https://doi.org/10.1007/s10973-015-5065-3.

Li, X.Y., Feng, J.C., Li, X.S., et al., 2022. Experimental study of methane hydrate formation and decomposition in the porous medium with different thermal conductivities and grain sizes. Appl. Energy 305, 117852. https://doi.org/10.1016/j.apenergy.2021.117852.

Liu, S., Liang, Y., Li, B., et al., 2019. Interaction relationship analysis between heat transfer and hydrate decomposition for optimization exploitation. Fuel 256, 115742. https://doi.org/10.1016/j.fuel.2019.115742.

Martinez de Baños, M.L., Carrier, O., Bouriat, P., et al., 2015. Droplet-based millifluidics as a new tool to investigate hydrate crystallization: insights into the memory effect. Chem. Eng. Sci. 123, 564–572. https://doi.org/10.1016/j.ces.2014.11.018.

Muraoka, M., Susuki, N., Yamaguchi, H., et al., 2015. Thermal properties of a supercooled synthetic sand–water–gas–methane hydrate sample. Energy Fuels 29 (3), 1345–1351. https://doi.org/10.1021/ef502350n.

Nagatomi, T., Taguchi, Y., Ohmura, R., et al., 2013. Thermal conductivity measurement of TBAB hydrate by the transient hot-wire using parylene-coated probe. Trans. Jap. Soc.Mech. Eng. 79 (802), 1155–1163. https://doi.org/10.1299/kikaib.79.1155.

Qin, X.W., Lu, C., Wang, P.K., et al., 2022. Hydrate phase transition and seepage mechanism during natural gas hydrates production tests in the South China Sea: a review and prospect. China Geol. 5, 201–217. https://doi.org/10.31035/cg2022029.

Ren, J., Liu, X., Niu, M., et al., 2022. Effect of sodium montmorillonite clay on the kinetics of CH_4 hydrate - implication for energy recovery. Chem. Eng. J. 437, 135368. https://doi.org/10.1016/j.cej.2022.135368.

Rosenbaum, E.J., English, N.J., Johnson, J.K., et al., 2007. Thermal conductivity of methane hydrate from experiment and molecular simulation. J. Phys. Chem. B 111 (46), 13194–13205. https://doi.org/10.1021/jp074419o.

Song, Y., Wang, J., Liu, Y., et al., 2016. Analysis of heat transfer influences on gas production from methane hydrates using a combined method. Int. J. Heat Mass Tran. 92, 766–773. https://doi.org/10.1016/j.ijheatmasstransfer.2015.08.102.

Sun, S., Gu, L., Yang, Z., et al., 2022. Thermophysical properties of natural gas hydrates: a review. Nat. Gas. Ind. B 9 (3), 246–263. https://doi.org/10.1016/j.ngib.2022.04.003.

Sun, S., Zhao, J., Zhao, J., et al., 2019. The effective thermal conductivity of methane hydrate-bearing seasand. J. Chem. Therm. 132, 423–431. https://doi.org/10.1016/j.jct.2019.01.023.

Touil, A., Broseta, D., Hobeika, N., et al., 2017. Roles of wettability and supercooling in cyclopentane hydrate spreading over a substrate. Langmuir 33 (41), 10965–10977. https://doi.org/10.1021/acs.langmuir.7b02121.

Wan, Q.C., Si, H., Li, B., et al., 2018. Heat transfer analysis of methane hydrate dissociation by depressurization and thermal stimulation. Int. J. Heat Mass Tran. 127, 206–217. https://doi.org/10.1016/j.ijheatmasstransfer.2018.07.016.

Wang, B., Fan, Z., Lv, P., et al., 2017. Measurement of effective thermal conductivity of hydrate-bearing sediments and evaluation of existing prediction models. Int. J. Heat Mass Tran. 110, 142–150. https://doi.org/10.1016/j.ijheatmasstransfer.2017.02.085.

Wei, R., Shi, K., Guo, X., et al., 2021. Evolving thermal conductivity upon formation and decomposition of hydrate in natural marine sediments. Fuel 302, 121141. https://doi.org/10.1016/j.fuel.2021.121141.

Wei, R., Xia, Y., Qu, A., et al., 2022. Dependence of thermal conductivity on the phase transition of gas hydrate in clay sediments. Fuel 317, 123565. https://doi.org/10.1016/j.fuel.2022.123565.

Wu, D., Li, S., Guo, Y., et al., 2022. A novel model of effective thermal conductivity for gas hydrate-bearing sediments integrating the hydrate saturation and pore morphology evolution. Fuel 324, 124825. https://doi.org/10.1016/j.fuel.2022.124825.

Xu, Z., Hu, T., Pang, X.Q., et al., 2022. Research progress and challenges of natural gas hydrate resource evaluation in the South China Sea. Petrol. Sci. 19 (1), 13–25. https://doi.org/10.1016/j.petsci.2021.12.007.

Yang, L., Zhao, J., Liu, W., et al., 2015. Experimental study on the effective thermal conductivity of hydrate-bearing sediments. Energy 79, 203–211. https://doi.org/10.1016/j.energy.2014.11.008.
Yang, L., Zhao, J., Wang, B., et al., 2016. Effective thermal conductivity of methane hydrate-bearing sediments: experiments and correlations. Fuel 179, 87–96. https://doi.org/10.1016/j.fuel.2016.03.075.
Yin, Z., Chong, Z.R., Tan, H.K., et al., 2016. Review of gas hydrate dissociation kinetic models for energy recovery. J. Nat. Gas Sci. Eng. 35, 1362–1387. https://doi.org/10.1016/j.jngse.2016.04.050.
Yin, Z., Linga, P., 2019. Methane hydrates: a future clean energy resource. Chin. J. Chem. Eng. 27 (9), 2026–2036. https://doi.org/10.1016/j.cjche.2019.01.005.
Yin, Z., Zhang, S., Koh, S., et al., 2020. Estimation of the thermal conductivity of a heterogeneous CH_4-hydrate bearing sample based on particle swarm optimization. Appl. Energy 271, 115229. https://doi.org/10.1016/j.apenergy.2020.115229.
Zhang, J., Liu, X., Chen, D., et al., 2022. An investigation on the permeability of hydrate-bearing sediments based on pore-scale CFD simulation. Int. J. Heat Mass Tran. 192, 122901. https://doi.org/10.1016/j.ijheatmasstransfer.2022.122901.
Zhang, P., Chen, X., Li, S., et al., 2021. Heat transfer and water migration rules during formation/dissociation of methane hydrate under temperature fields with gradient. Int. J. Heat Mass Tran. 169, 120929. https://doi.org/10.1016/j.ijheatmasstransfer.2021.120929.